Temperature Dependence of Thermal Boundary Resistances between Multiwalled Carbon Nanotubes and Some Typical Counterpart Materials

Guang Zhang, Changhong Liu,* and Shoushan Fan

Tsinghua-Foxconn Nanotechnology Research Center and Department of Physics, Tsinghua University, Beijing 100084, People's Republic of China

ABSTRACT

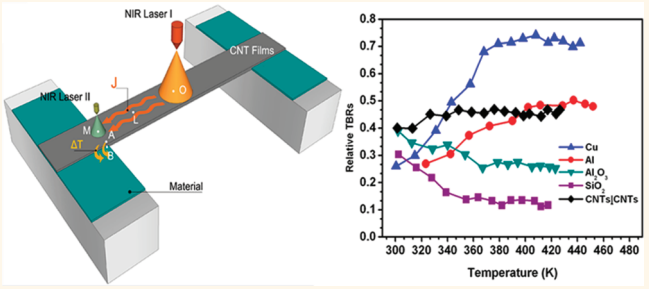

We directly measured the temperature dependence of thermal boundary resistances (TBRs) between multiwalled carbon nanotubes (MWCNTs) and different materials at elevated temperatures. Using the steady-state heat flow and the noncontacted measurement method, we could conveniently obtain the TBR—temperature relations. Our results indicate that the TBR—temperature relations vary distinctively with different contact materials when heating temperatures change from about 300 to 450 K; that is, the CNT—metal TBRs increase with increasing temperatures, whereas the CNT—insulator TBRs decrease. As a comparison, the TBRs between superaligned MWCNTs were measured and we found that the CNT—CNT TBRs remain basically unchanged as temperatures increase. We also found that the magnitude of TBRs between MWCNTs and different materials could differ from each other significantly. These results suggest that the choice of the right electrode may have an obvious influence on the thermal properties and other properties of the CNT-based devices. From another perspective, in view of some existing theoretical models about TBRs, our results support the validity of the molecular dynamics (MD) simulations in the calculation of CNT—solid TBRs at elevated temperatures.

KEYWORDS: thermal boundary resistances · carbon nanotubes · nanoscale devices · superaligned CNT films · heat transfer properties

Individual single-walled and multiwalled carbon nanotubes (CNTs) have very high thermal conductivity[1−5] and other outstanding properties. In recent years, micro/nanoscale devices based on CNTs have been widely studied.[6−9] A prominent example of these devices is the substrate-supported CNTs, where the CNT sidewall—plane contacts with electrodes or substrates. For example, Mann *et al.*[8] reported light emission from 10 suspended quasi-metallic single-walled CNTs, which is a result of thermal light emission owing to Joule heating in a one-dimensional system. For another example, Liu *et al.*[9] have demonstrated the first piezoelectric potential gated hybrid field-effect transistor based on single-walled nanotubes, where a single-walled nanotube was fabricated on a flexible substrate. These kinds of micro/nanoscale devices have very small size, and thus their thermal transport properties could seriously influence their behavior. Although individual CNTs and substrates could have outstanding intrinsic thermal properties, the CNT—substrate thermal boundary resistances (TBRs) are important energy barriers. So the TBRs between CNTs and substrates play a significant role in determining the thermal transport and other properties of these CNT-based devices. Individual CNTs or CNT bundles may be involved in the CNT-based devices. In addition to the CNT—substrate TBRs, TBRs between individual CNTs[10] could influence these devices' thermal properties and even limit further development of the CNT-based devices. For these reasons, it is necessary to determine the TBRs between CNTs and counterpart materials.

In our previous paper,[11] we carried out a noncontacted measurement to compare the relative TBRs of multiwalled carbon nanotubes (MWCNTs) in contact with metals and polymers at a specific temperature, where the MWCNTs have sidewall—plane contact conditions with counterpart materials. In this paper, we used the noncontacted method to investigate the temperature dependence of sidewall—plane contacted TBRs between MWCNTs and five typical

* Address correspondence to chliu@mail.tsinghua.edu.cn.

Received for review December 2, 2011 and accepted March 5, 2012.

Published online March 05, 2012
10.1021/nn204683u

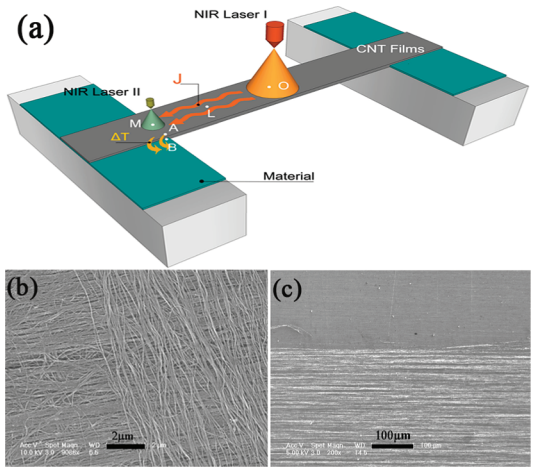

Figure 1. Measurement of the relative TBRs between MWCNTs and five typical materials. (a) Schematic graphics of the measurement. The NIR Laser I heated the CNT films and heat flow (*J*) transferred from CNT films to underlying materials. The NIR Laser II was employed to measure the temperatures of points L, M, A, and B. (b) Scanning electron microscope (SEM) images of the cross-contact condition between superaligned CNT films and superaligned buckypapers. (c) SEM images of the contact condition between superaligned CNT films and aluminum sheets.

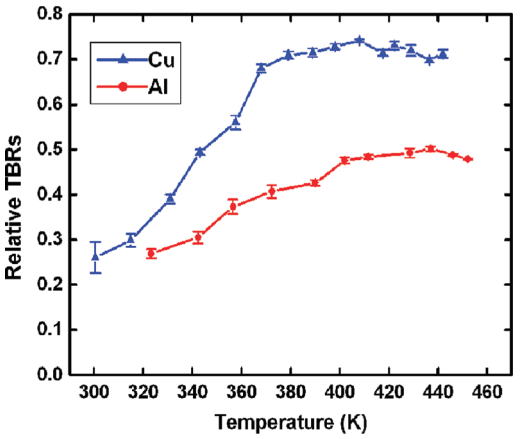

Figure 2. CNT/Al and CNT/Cu thermal boundary resistances as a function of temperatures. Each of them increases as the temperature increases from about 300 K and then reaches a plateau.

materials, that is, two metals, two insulators, and MWCNTs. Heating temperatures changed from about 300 to 450 K. Our results indicate that TBRs between MWCNTs and different typical materials have obviously different temperature dependence. We further suggest that the different temperature dependence originates from different thermal coupling mechanisms. In view of some existing theoretical models about TBRs, our results demonstrate that the molecular dynamics (MD) simulations[12−15] could well predict the CNT−insulator TBRs and that the electron−phonon coupling TBRs ($R_{e\text{-}p}$) may dominant CNT−metal TBRs at elevated temperatures.[16] Additionally, we found that the magnitude of TBRs between MWCNTs and different materials could differ from each other significantly. Reducing the TBRs at the interface is an available approach to improve the energy dissipation and transport in micro/nanoscale devices. Thus investigating the TBRs between MWCNTs and different materials is helpful for improving the thermal performance of CNT-based devices.

The MWCNTs used in our experiment were a kind of extremely lightweight (density is about 1.5 μg/cm^2) superaligned CNT films.[17] The diameters of these MWCNTs are about 10−20 nm, and the outside wall of these MWCNTs may be metallic or semiconductive, which depends on the exact diameter of the MWCNT. Five typical counterpart materials included two metals (aluminum, copper), two insulators (Al_2O_3, SiO_2), and the highly oriented buckypapers made of superaligned MWCNT arrays.[18] The thicknesses of the metal sheets, insulator slices, and buckypapers were 50 μm, 1.1 mm, and 20 μm, respectively. Two pieces of identical counterpart materials were adhered to a pair of aluminum substrates by the high-purity silver paste. The CNT films and buckypapers were both superaligned, so there were two contact conditions, that is, the cross-contact (Figure 1b) and the parallel-contact. In this way, we got six pairs of "thermal electrodes",[11] and the distance between two electrodes was 2.0 cm (Figure 1a). Then the superaligned continuous CNT films[19] were spread on the thermal electrodes and cut into 4 mm width ribbons by a high-power laser. The MWCNTs in the superaligned films lay flat on substrates and have a sidewall−plane contact condition with counterpart materials (Figure 1c). The contact length between MWCNTs and counterpart materials was much longer than individual MWCNTs. At last, an ethanol drop was dripped on joints to get sufficient contact conditions.

RESULTS AND DISCUSSION

The TBR is defined as $R_k = \Delta T/J$, where ΔT is the temperature drop and J is the heat flow at the interface.[20] It is very difficult to directly measure the temperature drop, so in this experiment, we chose two points (A on the CNTs films, B on the underlying materials) near the contacted interface and another two suspended points (L, M) on the CNT films to substitute the ΔT and J,[11] as is shown in Figure 1a. The points A and B were chosen as close to the interface as possible but on the films and underlying materials, respectively. Points L and M were 5 mm separated on suspended CNT films, and we need to ensure that they are fixed in every measurement. A near-infrared laser (Figure 1a, NIR Laser I) was used to heat the CNT sheets, and its central wavelength is 980 nm. We used an Optris LS infrared thermometer (Figure 1a, NIR Laser II) to collect the temperature data. This is a noncontacted thermometer, and its spatial and temperature resolution are 1 mm and 0.1 K, respectively. The precise position of the thermometer

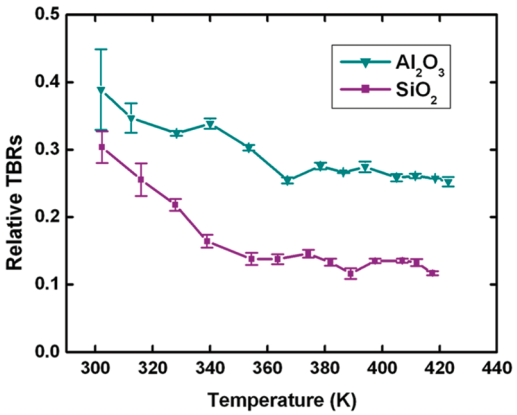

Figure 3. CNT/SiO_2 and CNT/Al_2O_3 thermal boundary resistances as a function of temperature. Both of them decrease as the temperature increases from about 300 K and then tend to relatively stable constants.

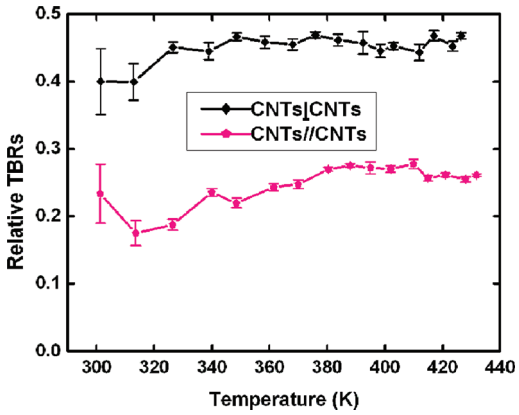

Figure 4. Temperature dependence of the cross-contact MWCNT TBRs and parallel-contact MWCNT TBRs. Both of them approximately remain unchanged as temperatures increase from 300 K. The TBRs between cross-contact CNTs have a larger value.

was controlled by a high-precision translation-and-lift stage. The microstructures of samples were probed by scanning electron microscopy (SEM; Sirion 200, resolution ~1.0 nm).

Heating temperatures of the suspended CNT films varied from approximately 300 to 450 K. The temperature drop (ΔT_{AB}) between A and B and the temperature difference (ΔT_{LM}) between L and M could be conveniently measured by the Optris LS infrared thermometer. The relative TBRs were determined by the ratio of ΔT_{AB} to ΔT_{LM}, that is, $R_k \sim \Delta T_{AB}/\Delta T_{LM}$[11] (for more deducing processes and error analysis details, readers can refer to ref 11 and Supporting Information). In this way, we obtained a series of TBRs as temperatures increase. Figures 2–4 show the temperature dependence of the six typical relative TBRs. The TBRs presented here are all relative values because of difficulties in determining the exact contact areas between MWCNTs and counterpart materials; this treatment is sufficient for comparison purposes discussed in this paper. Nevertheless, the exact TBR values and error analysis are given in the Supporting Information.

The temperature dependence of the CNT–metal TBRs is shown in Figure 2. The error bars capture the uncertainty due to variations in repeated measurement data. Heating temperature range was about 300–450 K, and the temperature drop between the CNT films and counterpart materials was about 1–5 K. This temperature range covers both the Debye temperatures (Θ_D) of aluminum ($\Theta_D \approx 428$ K) and copper ($\Theta_D \approx 340$ K). For the CNT/Cu interface, TBRs increase steadily as temperatures increase to approximately 370 K and then changes very mildly as temperatures further increase. The CNT/Al TBRs have a temperature dependence similar to that of CNT/Cu TBRs, but its turning temperature (~415 K) is higher than that of CNT/Cu. On the other hand, Figure 2 also shows that the value and the variation range of CNT/Al TBRs are both remarkably smaller than that of CNT/Cu TBRs. This result indicates that, in the sense of TBRs, the Al electrodes may perform better than Cu electrodes to improve the thermal properties of CNT-based devices.

There have been some reported works that studied the CNT (single-walled and multiwalled)–metal contact combination.[21−23] However, in the previous works, CNTs were mostly coated with metals or vertically synthesized on metals, where CNTs have top-end contact conditions with metals. For example, Panzer *et al.*[21] have separated the interface resistances for aligned single-walled carbon nanotube (SWCNT) films coated with Al, Ti, Pd, Pt, and Ni using nanosecond thermoreflectance thermometry. They further reported the temperature dependence of the interface resistance when the SWCNT top-end contacted with metals, which is a different result from this paper. Different from the previous studies, this work focuses on the sidewall–plane contact conditions between MWCNTs and metals. The phonon mode along the nanotube wall is obviously different from that at the nanotube end.

So far, we cannot completely clarify this MWCNT–metal thermal transfer mechanism. In this paper, we would just try to find some existing similar models of nonmetal–metal interface to explain our results. It is known that electrons dominate the heat transfer in metals, while it is phonons in nonmetals and CNTs. Li *et al.*[11] have shown that CNT–metal TBRs (R_k) consist of the electron–phonon coupling ($R_{e\text{-}p}$) and phonon–phonon coupling ($R_{p\text{-}p}$) constituents, that is, $R_k = R_{e\text{-}p} + R_{p\text{-}p}$. At sufficiently low temperatures, the $R_{p\text{-}p}$ dominates the R_k, and its temperature dependence is $R_{p\text{-}p} \sim 1/T^3$, whereas the $R_{e\text{-}p}$ can be ignored.[24] However, when temperatures are comparable to the Θ_D of metals, Majumdar *et al.*[16] suggested that the $R_{e\text{-}p}$ is comparable to the $R_{p\text{-}p}$ and thus cannot be ignored any more. They also suggested that the $R_{e\text{-}p}$ increases as $T^{1/2}$ and $R_{p\text{-}p}$ remain constant with increasing temperatures near the Θ_D.

In this case, the $R_{e\text{-}p}$ becomes more important and even dominant. Our measurements were carried out near the Θ_D of aluminum and copper, so the above-discussed theoretical models could provide support for our experimental results. Additionally, when temperatures are higher than the Θ_D of aluminum and copper, the R_k remains unchanged, as is shown in Figure 2. We suggest that this result may be due to the $R_{e\text{-}p}$ that also becomes independent of temperatures as temperatures further increase. More experimental and theoretical work is still needed in the future to clarify this suggestion.

The temperature dependence of the CNT−insulator TBRs is shown in Figure 3. For the CNT/SiO_2 and CNT/Al_2O_3 TBRs, they both decrease as temperatures increase from 300 K and then tend to a relatively stable constant. The turning temperature of CNT/SiO_2 is about 348 K, while that of CNT/Al_2O_3 is 367 K. These two types of TBRs have a similar temperature dependence which indicates that they have the same thermal coupling mechanisms. It is known that energy is primarily carried by phonons in insulators and CNTs.[11,25] So CNT−insulator TBRs mainly originate from the phonon−phonon coupling mechanism.

The CNT−insulator TBRs have been widely studied, and a number of results have been reported,[11,14,15,26,27] but the theoretical system is just beginning to take shape and much work remains to be done in this area. So far, there have been three reported theoretical models to calculate the phonon−phonon coupling TBRs: the acoustic mismatch models (AMM),[28,29] the diffuse mismatch models (DMM),[24] and the molecular dynamics (MD) simulations.[12−15] The AMM and DMM are based on continuum models, which only consider the elastic phonon scattering at the interface and ignore the inelastic ones. This treatment is sufficient at low temperatures, but the inelastic phonon scattering will become intensive as temperatures increase. Therefore, either AMM or DMM can well predict the solid−solid TBRs only at very low temperatures (<30 K).[24] By contrast, the MD simulations are derived from the interaction of atoms and inelastic phonon scattering at the interface. Given this, it may be a more effective model to calculate the solid−solid TBRs at elevated temperatures. Using the MD simulations, Ong *et al.*[14] obtained the temperature dependence of the CNT/SiO_2 TBRs as $R_k \sim T^{-1/3}$ (between 200 and 600 K), and they also found that the high-frequency (40−57 THz) CNT phonons have very small contribution to the interfacial heat transfer,[15] which means that when interfacial temperatures exceed a typical temperature, TBRs will not significantly change with temperature. These results derived from the MD simulations are different from that derived from the AMM or DMM but have a good correspondence with the results of this paper.

The CNT/Al_2O_3 TBRs have similar temperature dependence with that of CNT/SiO_2, as is shown in Figure 3.

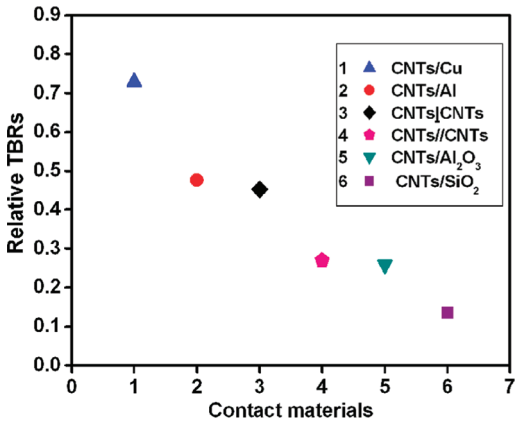

Figure 5. Magnitude of relative TBRs between CNTs and six typical substrates at 400 K.

This result may be also attributed to the phonon−phonon coupling mechanism. The temperature dependence of the two typical CNT−insulator TBRs reported here suggest that, at the mechanism of phonon−phonon coupling interfacial thermal transport, the inelastic scattering plays an important role and cannot be ignored at elevated temperatures. Because the AMM and DMM ignore the role of inelastic scattering, the MD simulations will work more effectively than AMM and DMM above room temperature. Finally, it is worth noting that CNT/Al_2O_3 TBRs are significantly higher than CNT/SiO_2 at the same temperatures, as is shown in Figure 3. Nowadays, we cannot exactly explain this result, and more experimental and theoretical work is needed in the future.

There were two contact conditions between the superaligned CNT films and superaligned buckypapers: the cross-contact (CNTs⊥CNTs) and parallel-contact (CNTs//CNTs). Thus, we obtained two series of TBRs between MWCNTs, and their temperature dependences are shown in Figure 4. These curves indicate that TBRs between MWCNTs remain basically unchanged as temperatures increase from 300 K. This is an obviously different temperature dependence from that of CNT−metal and CNT−insulator TBRs, and it has a good agreement with findings of Yang *et al.*,[10] which derived the TBRs between two individual MWCNTs with temperature changes from about 50 to 400 K. Another interesting result is that the magnitude of the CNTs⊥CNTs TBRs is about two times higher than that of CNTs//CNTs TBRs above room temperature. The smaller TBRs between the parallel-contact MWCNTs may be due to the bigger contact areas and more phonon coupling modes because of a similar phonon mode along the tube wall. These reported results demonstrate that the superparallel structure in CNT-based devices could highly enhance their thermal properties.

Finally, the magnitudes of the six discussed TBRs at a specific temperature (400 K) are shown in Figure 5. The sizes of the symbols capture the uncertainty due to variations in repeated measurement data. This figure

clearly demonstrates that the CNT−metal contact has the largest TBRs at 400 K, which could be attributed to the small phonon mode overlapping and the strong phonon scattering at the interface.[11] Figure 5 also shows that the CNT−CNT contacts give higher TBRs than the CNT−insulator contacts at this specific temperature; this is a novel phenomenon and a different result derived from the AMM. According to the AMM, the same kind of materials may have the lowest TBRs due to the largest phonon mode overlapping. Thus, this result may suggest that the TBRs also arise from other mechanisms besides the phonon mismatch model.

As mentioned before, the CNT-based devices may have very small size and thus their thermal transport properties could seriously influence their behavior. Therefore, when choosing electrode materials of the CNT-based devices, we should take into account both the electric conductivity and the thermal transport properties. Figure 5 shows that CNT/SiO_2 has the smallest TBRs among the five typical materials at the temperature 400 K, but SiO_2 has very poor electric conductivity. On the other hand, metals like Cu and Al may have good electric conductivity, but their TBRs when contacted with CNTs are much bigger than other materials. Thus, to sum up the points which we have just indicated, the graphite and other carbon-based materials may be the best electrode materials for the CNT-based devices at this temperature.

CONCLUSION

In summary, we directly measured the relative TBRs between MWCNTs and five different typical materials above room temperature. By changing heating temperatures, we obtained the temperature dependence of the five typical TBRs. Our results indicate that TBRs of different kinds of contacted materials have different temperature dependence. Then we suggest that these results originate from different thermal coupling mechanisms. For the CNT−metal TBRs, owing to the important role of the electron−phonon coupling above room temperature, they monotonously increase as temperatures increase from about 300 K. For the CNT−insulator TBRs, because the inelastic phonon scattering at the interface cannot be ignored at high temperatures, they monotonously decrease as temperatures increase. We also found that the TBRs between MWCNTs remain basically unchanged as temperatures increase, and the parallel-contact MWCNTs have lower TBRs than the cross-contact MWCNTs. These results of TBRs between MWCNTs and different materials reported here are helpful for improving the thermal performance of CNT-based devices. From another perspective, our results support the validity of the MD simulations in the calculations of CNT−solid TBRs at elevated temperatures.

METHODS

Preparation of the "Thermal Electrodes" and Properties of Superaligned CNT Films. Substrates used in this experiment are 6 cm × 1.4 cm × 1.2 cm aluminum blocks. The five typical materials had smooth surface and were cut into the same size with the aluminum substrates. Two pieces of each material were adhered to a pair of substrates by high-purity silver paste in order to get a perfect heat transfer condition. Then superaligned CNT films were drowned out from the superaligned CNT arrays. The superaligned CNT arrays were synthesized on silicon wafers in a low-pressure chemical vapor deposition (LP-CVD) system.[19] In order to lessen the tube−tube TBRs, the CNT films were ultrathin and approximately single-layer.

Precise Position Control of the Measurement Points. We chose four separate points to calculate relative TBRs in this experiment. These points must be precisely controlled and ensured to have the same position for every material. A high-precision translation-and-lift stage was used to ensure the precise position control, where it can move in three-dimensions and the spatial resolution is 0.01 mm. Point M was chosen on the suspended CNT films and is very close to the contact interface, and the distance apart from the edge is 0.5 mm, as is shown in Figure 1a. Another suspended point L was 5 mm apart from point M. Points A and B were chosen on the CNT films and on the material, respectively. The temperature difference between A and B (ΔT_{AB}) substitutes the temperature drop (ΔT) at the interface, so these two points were chosen as closely as possible to the contact interface for the purpose of reducing the inaccuracy (detailed analysis indicated in ref 11).

Conflict of Interest: The authors declare no competing financial interest.

Acknowledgment. This work was supported by National Basic Research Program of China (2012CB932301) and the National Natural Science Foundation of China (51173098, 10721404).

Supporting Information Available: Additional information for deducing processes of equations; exact values of TBRs; error analysis details. This material is available free of charge *via* the Internet at http://pubs.acs.org.

REFERENCES AND NOTES

1. Yang, J.; Yang, Y.; Waltermire, S. W.; Gutu, T.; Zinn, A. A.; Xu, T. T.; Chen, Y.; Li, D. Measurement of the Intrinsic Thermal Conductivity of a Multiwalled Carbon Nanotube and Its Contact Thermal Resistance with the Substrate. *Small* **2011**, *7*, 2334–2340.
2. Pop, E.; Mann, D.; Wang, Q.; Goodson, K.; Dai, H. Thermal Conductance of an Individual Single-Wall Carbon Nanotube above Room Temperature. *Nano Lett.* **2006**, *6*, 96–100.
3. Kim, P.; Shi, L.; Majumdar, A.; Mceuen, P. L. Thermal Transport Measurements of Individual Multiwalled Nanotubes. *Phys. Rev. Lett.* **2001**, *87*, 215502.
4. Li, Q. W.; Liu, C. H.; Wang, X. S.; Fan, S. S. Measuring the Thermal Conductivity of Individual Carbon Nanotubes by the Raman Shift Method. *Nanotechnology* **2009**, *20*, 145702.
5. Choi, T.; Poulikakos, D.; Tharian, J.; Sennhauser, U. Measurement of the Thermal Conductivity of Individual Carbon Nanotubes by the Four-Point Three-ω Method. *Nano Lett.* **2006**, *6*, 1589–1593.
6. Zhou, W.; Bai, X.; Wang, E.; Xie, S. Synthesis, Structure, and Properties of Single-Walled Carbon Nanotubes. *Adv. Mater.* **2009**, *21*, 4565–4583.

7. Zhang, L.; Tu, X. M.; Welsher, K.; Wang, X. R.; Zheng, M.; Dai, H. J. Optical Characterizations and Electronic Devices of Nearly Pure (10,5) Single-Walled Carbon Nanotubes. *J. Am. Chem. Soc.* **2009**, *131*, 2454.
8. Mann, D.; Katoy, K.; Kinkhabwala, A.; Pop, E.; Cao, J.; Wang, X.; Zhang, L.; Wang, Q.; Guo, J.; Dai, H. Electrically Driven Thermal Light Emission from Individual Single-Walled Carbon Nanotubes. *Nat. Nanotechnol.* **2007**, *2*, 33–38.
9. Liu, W.; Lee, M.; Ding, L.; Liu, J.; Wang, Z. L. Piezopotential Gated Nanowire−Nanotube Hybrid Field-Effect Transistor. *Nano Lett.* **2010**, *10*, 3084–3089.
10. Yang, J. K.; Waltermire, S.; Chen, Y. F.; Zinn, A. A.; Xu, T. T.; Li, D. Y. Contact Thermal Resistance between Individual Multiwall Carbon Nanotubes. *Appl. Phys. Lett.* **2010**, *96*, 023109.
11. Li, Q. W.; Liu, C. H.; Fan, S. S. Thermal Boundary Resistances of Carbon Nanotubes in Contact with Metals and Polymers. *Nano Lett.* **2009**, *9*, 3805–3809.
12. Carlborg, C. F.; Shiomi, J.; Maruyama, S. Thermal Boundary Resistance between Single-Walled Carbon Nanotubes and Surrounding Matrices. *Phys. Rev. B* **2008**, *78*, 205406.
13. Zhong, H.; Lukes, J. R. Interfacial Thermal Resistance between Carbon Nanotubes: Molecular Dynamics Simulations and Analytical Thermal Modeling. *Phys. Rev. B* **2006**, *74*, 125403.
14. Ong, Z.; Pop, E. Molecular Dynamics Simulation of Thermal Boundary Conductance between Carbon Nanotubes and SiO_2. *Phys. Rev. B* **2010**, *81*, 155408.
15. Ong, Z.; Pop, E. Frequency and Polarization Dependence of Thermal Coupling between Carbon Nanotubes and SiO_2. *J. Appl. Phys.* **2010**, *108*, 103502–103508.
16. Majumdar, A.; Reddy, P. Role of Electron−Phonon Coupling in Thermal Conductance of Metal−Nonmetal Interfaces. *Appl. Phys. Lett.* **2004**, *84*, 4768–4770.
17. Jiang, K. L.; Li, Q. Q.; Fan, S. S. Spinning Continuous Carbon Nanotube Yarns. *Nature* **2002**, *419*, 801.
18. Wang, D.; Song, P. C.; Liu, C. H.; Wu, W.; Fan, S. S. Highly Oriented Carbon Nanotube Papers Made of Aligned Carbon Nanotubes. *Nanotechnology* **2008**, *19*, 07569.
19. Zhang, X. B.; Jiang, K. L.; Teng, C.; Liu, P.; Zhang, L.; Kong, J.; Zhang, T. H.; Li, Q. Q.; Fan, S. S. Spinning and Processing Continuous Yarns from 4-Inch Wafer Scale Super-Aligned Carbon Nanotube Arrays. *Adv. Mater.* **2006**, *18*, 1505.
20. Kapitza, P. L. The Study of Heat Transfer in Helium II. *J. Phys. USSR* **1941**, *4*, 181–210.
21. Panzer, M. A.; Duong, H. M.; Okawa, J.; Shiomi, J.; Wardle, B. L.; Maruyama, S.; Goodson, K. E. Temperature-Dependent Phonon Conduction and Nanotube Engagement in Metalized Single Wall Carbon Nanotube Films. *Nano Lett.* **2010**, *10*, 2395–2400.
22. Panzer, M. A.; Zhang, G.; Mann, D.; Hu, X.; Pop, E.; Dai, H.; Goodson, K. E. Thermal Properties of Metal-Coated Vertically Aligned Single-Wall Nanotube Arrays. *J. Heat Transfer* **2008**, *130*, 52401–52409.
23. Cola, B. A.; Xu, J.; Cheng, C.; Xu, X.; Fisher, T. S.; Hu, H. Photoacoustic Characterization of Carbon Nanotube Array Thermal Interfaces. *J. Appl. Phys.* **2007**, *101*, 54313.
24. Swartz, E. T.; Pohl, R. O. Thermal-Boundary Resistance. *Rev. Mod. Phys.* **1989**, *61*, 605–668.
25. Dresselhaus, M. S.; Eklund, P. C. Phonons in Carbon Nanotubes. *Adv. Phys.* **2000**, *49*, 705.
26. Pop, E. Energy Dissipation and Transport in Nanoscale Devices. *Nano Res.* **2010**, *3*, 147–169.
27. Nan, C. W.; Liu, G.; Lin, Y. H.; Li, M. Interface Effect on Thermal Conductivity of Carbon Nanotube Composites. *Appl. Phys. Lett.* **2004**, *85*, 3549–3551.
28. Khalatnikov, I. M. Teploobmen Mezhdu Tverdym Telom i Geliem-II. *Zh. Eksp. Teor. Fiz.* **1952**, *22*, 687–704.
29. Little, W. A. The Transport of Heat between Dissimilar Solids at Low Temperatures. *Can. J. Phys.* **1959**, *37*, 334–349.